17th World Conference on Earthquake Engineering, 17WCEE
Sendai, Japan - September 13th to 18th 2020

NUMERICAL SIMULATION ON THE SEISMIC RESPONSE OF A TEACHING BUILDING IN THE CHANGNING MS6.0 EARTHQUAKE

ZP. Shao (1), JW. Dai (2), W. Bai (3), YQ. Yang (4), DF. Xu (5)

(1) *Master student, Institute of Engineering Mechanics, China Earthquake Administration, 29 Xuefu Road, Harbin, Heilongjiang, China, 150080, e-mail: 772842315@qq.com*
(2) *Professor, Institute of Engineering Mechanics, China Earthquake Administration,29 Xuefu Road, Harbin, Heilongjiang, China, 150080, e-mail: jwdai@iem.cn*
(3) *Assistant professor, Institute of Engineering Mechanics, China Earthquake Administration, 29 Xuefu Road, Harbin, Heilongjiang, China, 150080, e-mail: 781090853@qq.com*
(4) *Assistant professor, Institute of Engineering Mechanics, China Earthquake Administration, 29 Xuefu Road, Harbin, Heilongjiang, China, 150080, e-mail: yangiem@foxmail.com*
(5) *Ph.D student, Institute of Engineering Mechanics, China Earthquake Administration, 29 Xuefu Road, Harbin, Heilongjiang, China, 150080, e-mail: xudefeng_2008@126.com*

Abstract

In recent years, the seismic damage as well as the safety consequences of the non-structural components of buildings have aroused extensive attention to academy, industry and even the government. In the 2017 China Jiuzhaigou Ms7.0 earthquake, totally 9 of 29 deaths were killed by the collapse of nonstructural components. Even in smaller events such as the only 2 deaths in the 2019 Rongxian Ms4.9 earthquake, and the only 1 death in the 2019 Weiyuan Ms5.4 earthquake, were all killed by the collapse of the parapet wall of multi-story buildings without any seismic measurement. In the Changing Ms6.0 earthquake occurred on June 17, 2019, in Sichuan Province of China southwestern, this phenomenon caused serious concern to the investigators again because of the non-structural damage everywhere in the affected area. Quite few of local public buildings in terms of school, hospital and government office buildings constructed with masonry infill RC frame structures lost their functions due to the severe damage of masonry infills, ceilings and facilities instead of structural damages. Even though, buildings with good seismic performances of non-structural components in the earthquake still be observed in the epicenter area of Changing Ms6.0 earthquake. As one of the good examples, a four-story teaching building in a local primary school constructed with masonry infilled RC frame structure, about 12 Km west to the epicenter, only very light damage of the nonstructural components such as the masonry infills and ceilings were observed.

For better understanding to the seismic performance of the example teaching building lightly damaged abovementioned, two integrated finite element (FE) models in considering both of the structure and the masonry infills are established in this paper, the first is built by solid element and the second is built by beam and shell element. The accuracy and the reasonability of the FE model is validated with the test results of ambient vibration tests carried out on-site for the teaching building after the earthquake. Nonlinear numerical simulations to the seismic responses of the teaching building were performed with the acceleration time histories recorded in the main-shock and after-shocks at the strong ground motion station about 1800 meters away from the teaching building. Comparisons between the numerical results and the reconnaissance observations to the masonry infills are discussed. The story relative displacement results of the solid FE model response spectrum analysis and the elastoplastic time history analysis were compared.

Keywords: Changning Ms6.0 earthquake, seismic response, finite element simulation, frame structure, masonry infills

1. Introduction

Frame structure is defined by the connection of beams and columns in the form of rigidity or hinge, and is the simplest structure bearing system that can bear the external force. It is widely used in public buildings such as residential buildings and office buildings. In China, reinforced concrete frame structure is widely used in civil buildings due to its advantages of good space flexibility and relative saving of concrete.[1]

For moderate intensity earthquake events, the damage to the frame structures is mainly concentrated in the serious damage to masonry infills, ceilings and facilities instead of structural damages, and only a few buildings lose their use function, such as the Jiuzhaigou 7.0 earthquake in 2017 and the Weiyuan 5.4 earthquake in 2019. Therefore, it is necessary to study the aseismic behavior of frame structures. In the Changing Ms6.0 earthquake occurred on June 17, 2019, in Sichuan Province of China, this phenomenon caused serious concern to the investigators again because of the non-structural damage everywhere in the affected area. The survey results show that most of the frame structures in this earthquake are public buildings, which were designed and constructed formally. During this earthquake, the beams and columns of the frame structure were damaged slightly, while the infilled wall and parapet are seriously damaged, especially, the hollow brick infilled wall and aerated concrete block infilled wall were severely damaged. The cross type through diagonal cracks or collapses are commonly found, some parapets are cracked or even collapsed, and the decoration works are seriously damaged. However, there are still a few frame structures performed well, as a good example, the teaching building of a primary school, about 12 Km west to the earthquake epicenter, only very light damage of the nonstructural components such as the masonry infills and ceilings were observed.

For better understanding the seismic performance of the example teaching building lightly damaged abovementioned, two integrated finite element (FE) models in considering all the components are built. In the first FE model, the beams, columns and slabs of the frame structure are modeled by solid element with dispersion reinforcement, and the masonry infills are modeled as a whole by solid element; in the second FE model, the beams and columns are modeled by beam element and the slabs and masonry infills are modeled by shell element. In the two models, the same constitutive relation is adopted. The picture of this teaching building can be seen at Fig.1.

Fig.1 – Picture of the teaching building.

Nonlinear numerical simulations to the seismic responses of the teaching building were performed with the acceleration time histories recorded in the main-shock and after-shocks at the strong ground motion station about 1800 meters away from the teaching building. The story relative displacement results of the solid FE model response spectrum analysis and the elastoplastic time history analysis were compared.

2. General information of the teaching building

The teaching building is about 12 km away from the epicenter, covering an area of 1100 m^2, with a total building area of 4400 m^2. The structural form is a four-story full frame cast-in-place reinforced concrete structure, with a total building height of 15.6 m. The design intensity of the teaching building is 6 degrees (0.05g). The teaching building is divided into three parts, separated by 100 mm separation gaps, and the largest part of the teaching building was selected to establish the FE model. The picture of the part selected to establish the FE model can be seen at Fig.2.

The part of the teaching building selected to establish the FE model is the largest part with the length of 48.6 m and the width of 8.7 m. The height of each floor is 3.6 m, and the total height is 15.6m with the 1.2 m high parapet on the top roof. The beam-column structure diagram of the selected part can be seen at Fig.3.

Fig.2 – Modeling part of the teaching building.

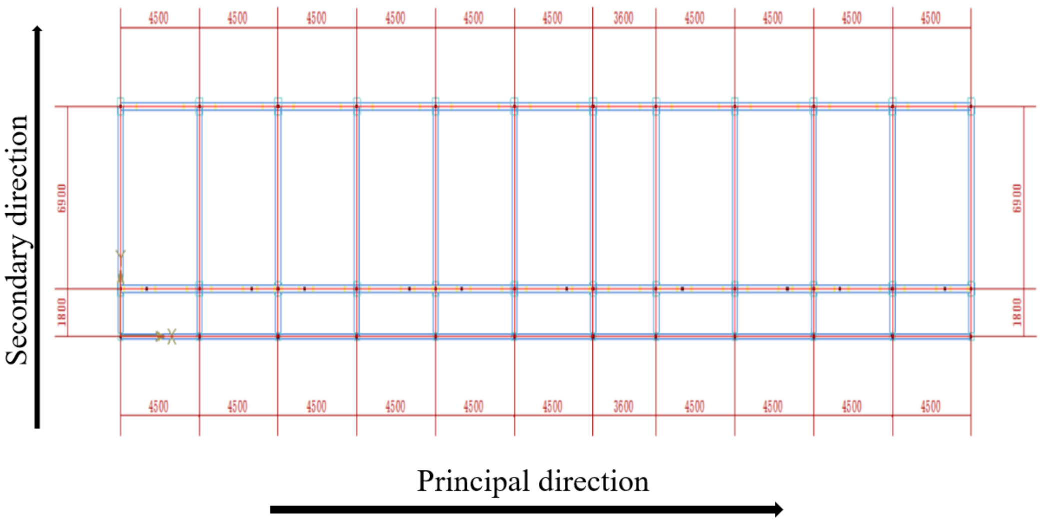

Fig.3 – The beam-column structure diagram of the modeling part

The masonry infills are made of 200 mm rectangular porous brick, the strength grade of brick masonry is MU10, and the strength grade of mortar is M5. The concrete grade of all cast-in-place beams, columns and slabs is C30, and the thickness of each floor slab is 120 mm. The reinforcement grade of beams and columns is HRB335, and the reinforcement grade of slabs is HPB235.

3. Establishment of the Solid Integrated Finite Element (FE) Model

Two integrated finite element (FE) models were established. The one was established by solid element and the other one was established by beam and shell element, and the same material constitutive relations were adopted. In this paper, only the establishment process of solid FE model was introduced.

3.1 Numerical geometry model

According to the characteristics of the finite element analysis software, the modeling methods can be divided into two categories: 1) direct modeling and 2) numerical geometry modeling to generate the finite element model [2-5]. Direct modeling is only applicable to simple and small models, which are composed of nodes and elements directly. While, the other method, firstly establish numerical geometric model, and then generate finite element model by meshing, could be applied to relatively complex 3D solid analysis model.

In order the establish the complex FE model of the teaching building, the method of numerical geometry modeling to generate the finite element model was used and the geometric numerical model should be established firstly. The underground portion of the building, all stairs and parapets were not considered in the FE model. The geometric numerical model can be seen at Fig.4.

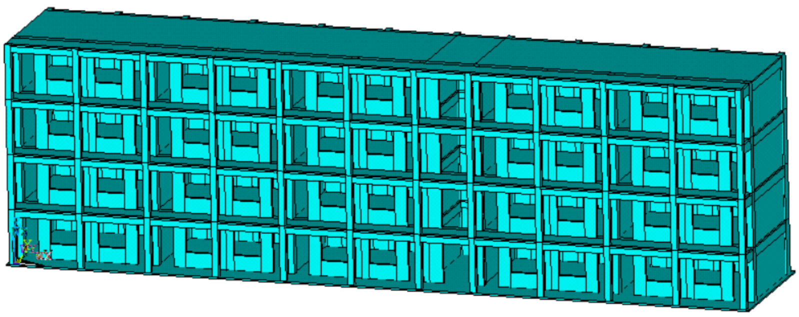

Fig.4 – Numerical geometry model of the modeling part.

3.2 Simulation of reinforced concrete structural components

3.2.1 Finite element modeling methods

The reinforced is composed of two materials: concrete and reinforcement. At present, three kinds of finite element modeling methods for reinforced concrete are commonly used: integral, combined and separated [6].

The integral modeling method is usually used in the case of large model and limitation of computer condition. It is considered that the reinforcement dispersed in concrete and the reinforcement is well bonded with concrete. Therefore, the reinforced concrete could be assumed as a continuous and homogeneous material. The disadvantage is that the internal force of the reinforcement cannot be obtained. Compared with integral method, the other two methods have higher requirements for the computer and is often used in the study of micro stress in the components.

As the reason that internal force of reinforced concrete members is not the main research content and the limitation of computer, integral modeling method was used to establish the solid FE model.

3.2.2 Element selection

Solid 65 element was selected to simulate reinforced concrete members [7]. The solid 65 element is consisted of two parts: one is the same solid element as the general 8-node spatial solid element solid 45, but the three-dimensional strength criterion of concrete is added; the other is the integral reinforcement model composed of dispersion reinforcement elements, which can set the position, angle, reinforcement ratio and other parameters of reinforcement in different directions of three-dimensional space. The solid 65 geometry can be seen at Fig.5.

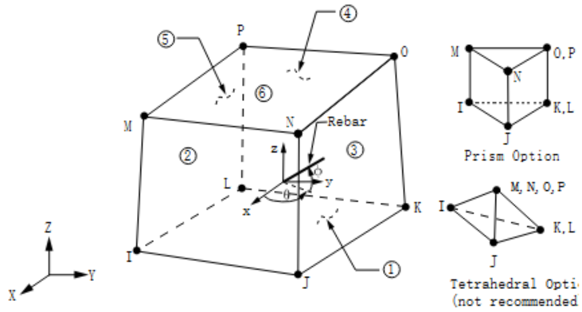

Fig.5 – Solid 65 geometry [8]

3.2.3 Material constitutive relation

According to the Code for design of concrete structures [9] of China, the material constitutive relation of reinforcement and concrete was given. Reinforcement adopted bilinear strengthening model (Fig.6), and concrete adopted multilinear strengthening model (Fig.7). The detailed data of the two material constitutive relation can be seen at Table 1 and Table 2.

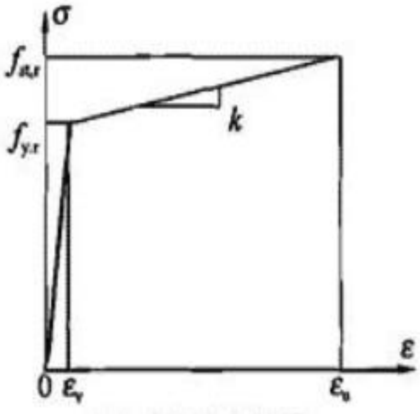

Fig.6 – bilinear strengthening model [9]

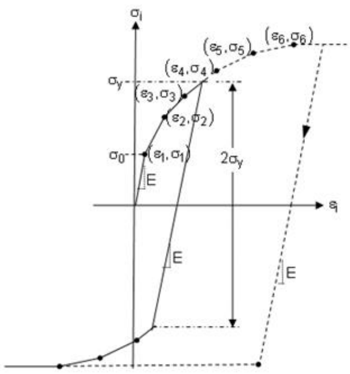

Fig.7 – multilinear strengthening model [8]

Table 1 – Constitutive relation data of the reinforcement (N/mm^2) [9]

Reinforcement	**Elastic modulus(E)**	**Yield strength (f_y)**	**Tangent modulus(k)**
HRB335	2.0×10^5	335	1600
HPB235	2.1×10^5	235	1350

Table 2 – Constitutive relation data of the C30 concrete [9]

I	1	2	3	4	5
Strain (ε_i)	0.0005	0.001	0.0015	0.002	0.003
Stress(σ_i)(N/mm^2)	15	21	24	27	27

3.3 Simulation of the masonry infills

3.3.1 Finite element modeling methods

In addition to the equivalent diagonal strut model, three methods of masonry infills simulation are commonly used: 1) consider the masonry infills as the homogeneous material, and consider the influence of the mortar joint in the mean sense; 2) simulate the masonry block with the continuum element, and the mortar joint with the interface element; 3) simulate the masonry block and the mortar joint with the continuum element. [9~10]

The method of considering the masonry infills as the Homogeneous material was used. The average strength of masonry infills (f_m) is determined by Eq. (1). [11]

$$f_m = k_1 f_1^{\alpha}(1 + 0.07 f_2) k_2 \quad (1)$$

In Eq. (1), f_1 is the strength grade of masonry block (10MPa); f_2 is the average compressive strength of mortar (5MPa); $k_1 = 0.78$;$\alpha = 0.5$;$k_2 = 1$.

3.3.2 Element and material constitutive relation

As the masonry infills was considered as a homogeneous material, solid 65 without integral reinforcement can be used. Multilinear strengthening model (Fig.7) was adopted, and the data can be seen at Table 3.

Table 3 – Constitutive relation data of the masonry infills [10]

I	1	2	3	4	5
Strain (ε_i)	0.0005	0.001	0.0015	0.0024	0.003
Stress(σ_i)(N/mm^2)	1.22	2.16	2.83	3.22	3.22

3.4 The element division of FE model

The element size is defined as 100 mm, the total number of nodes in the whole FE model is 684440, and the total number of the element is 1091490. The FE meshing details can be seen at Fig.8.

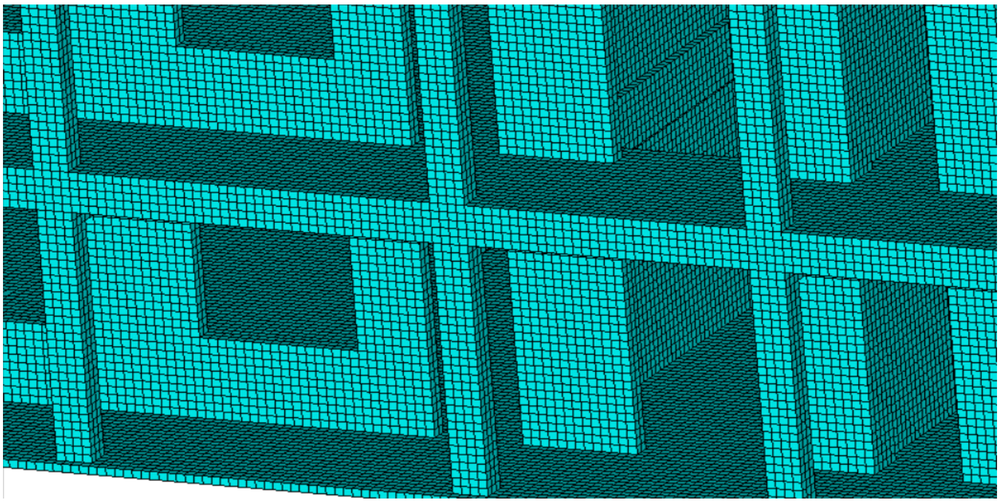

Fig.8 – FE meshing details

4. Ground Motion Information

The ground motion data recorded by the station closest to the teaching building was selected for the nonlinear numerical simulations to the seismic responses of the integrated FE model. The recorded acceleration and the spectra of the ground motion selected can be seen at Fig.9—Fig16. The peak value of ground motion in EW direction is 599.37 cm/s^2; in NS direction is -499.013 cm/s^2; in UD direction is -414.6530 cm/s^2.

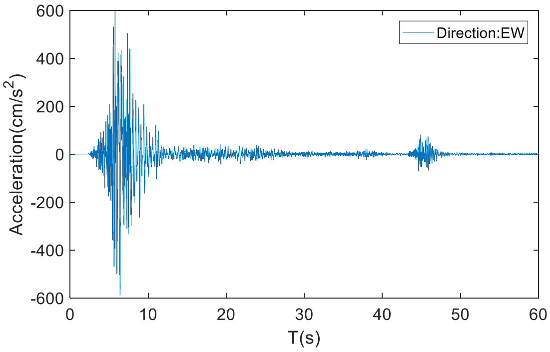

Fig.9 – Ground motion in the EW direction

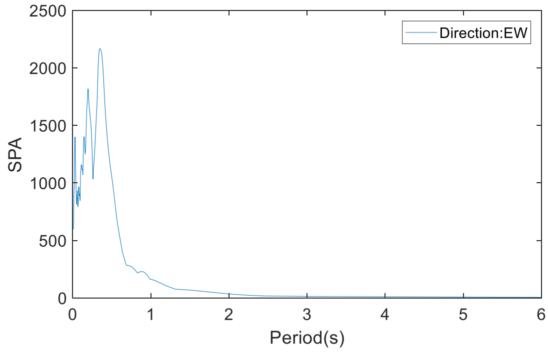

Fig.10 – Spectra of ground motion in the NS direction

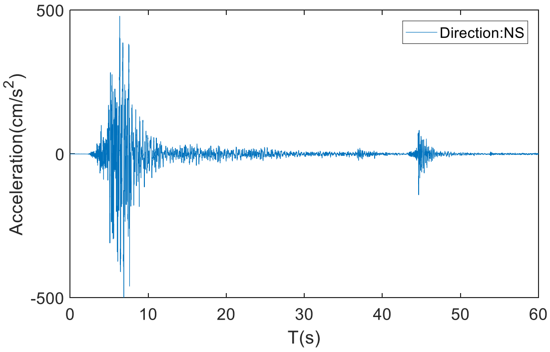

Fig.11 – Ground motion in the NS direction

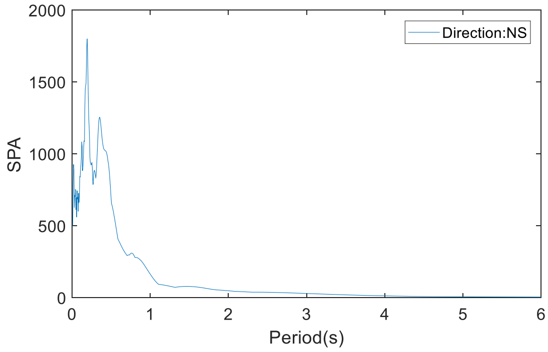

Fig.12 – Spectra of ground motion in the NS direction

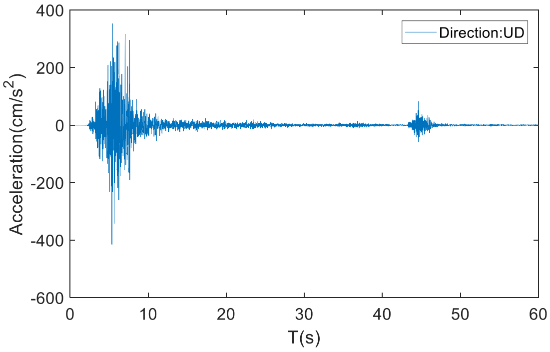

Fig.13 – Ground motion in the UD direction

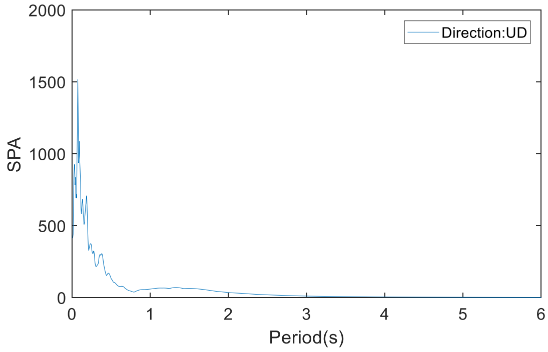

Fig.14 – Spectra of ground motion in the UD direction

5. Analysis Result

5.1 Modal analysis results

Six modes are calculated with the solid FE model in modal analysis, and related periods are listed in Table 4. Modal shapes of the first three mode can be seen at Fig.14 – Fig.17.

Table 4 – Constitutive relation data of the masonry infills [12]

Modal	1	2	3	4	5	6
Frequency(s^{-1})	2.6457	3.4962	3.6481	7.7110	8.1630	8.2876
Period(s)	0.3780	0.2860	0.2741	0.1297	0.1225	0.1207

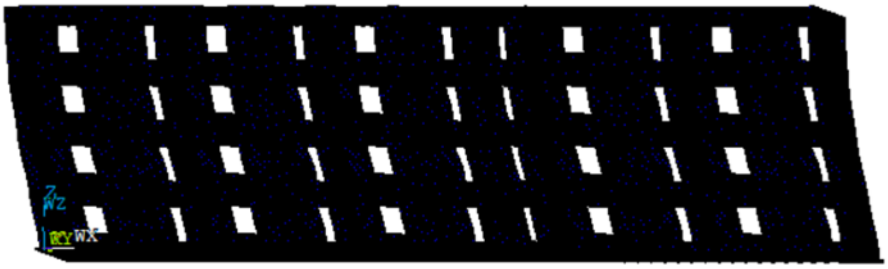

Fig.15 – First mode diagram (horizontal 1)

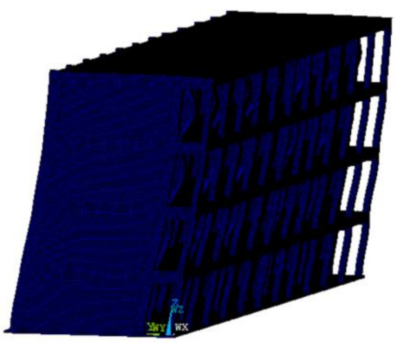

Fig.16 – Second mode diagram (horizontal 2)

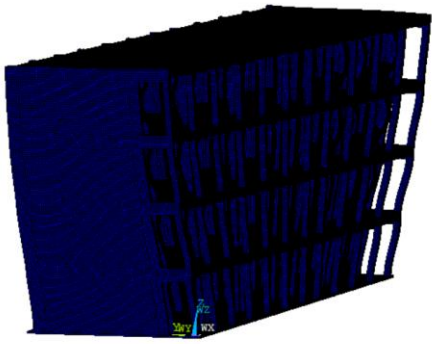

Fig.17 – Third mode diagram (rotational)

5.2 Response spectrum analysis

According to the calculated modal results and the response spectrum information of the ground motion, the response spectrum analysis of the model was carried out, and the SRSS method is used for combination. The displacement in the long axis direction of teaching building can be seen at Fig.18.

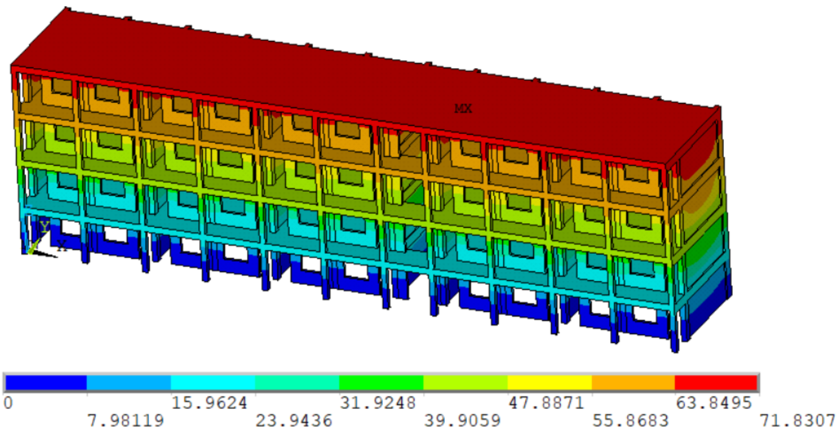

Fig.18 – Displacement in the principal direction (mm)

5.3 Elastoplastic time history analysis results

Due to the limitation of computer condition, elastoplastic time history analysis was calculated by the beam-shell FE model. The long axis direction of the teaching building is considered as the principal direction, and the short axis direction of the structure is considered as the secondary direction (Fig.19).

As the failure of infilled walls is controlled by displacement, masonry infills in four positions were selected to output the story relative displacement analysis results: (A) side masonry infills vertical to the principal direction; (B) side masonry infills (Near the corridor) Parallel to the principal direction; (C) middle masonry infills vertical to the principal direction; (D) middle masonry infills (Near the corridor) Parallel to the principal direction. The location of masonry infills with output story relative displacement can be seen at Fig.19.

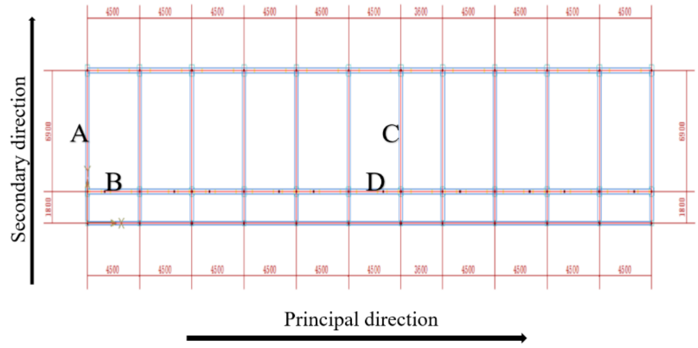

Fig.19 – The location of selected masonry infills

The story relative displacement of each floor was output, and the direction of story relative displacement is determined by the masonry infills, for masonry infills in position (B) and (D), story relative displacement in the principal direction was outputted and for masonry infills in position (A) and (C), story relative displacement in the secondary direction was outputted. The story relative displacement analysis results can be seen at Fig.20 -- Fig.23.

Compared with the principal direction, the story relative displacement in the principal direction is obviously larger, which is consistent with the actual earthquake damage of the teaching building. The actual earthquake damage of the masonry infills can be seen at Fig.24 -- Fig.25.

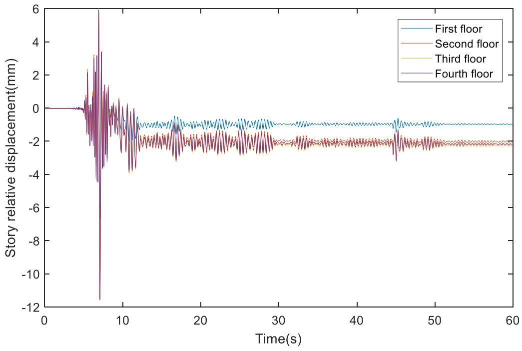

Fig.20 – Story relative displacement of masonry infill (A)

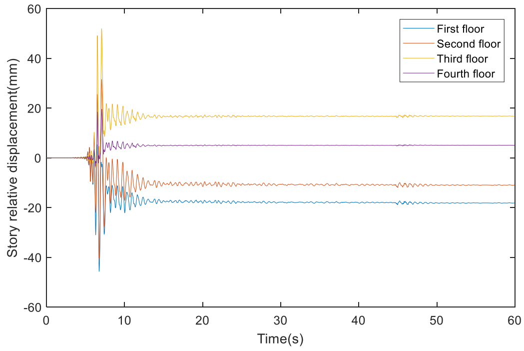

Fig.21 – Story relative displacement of masonry infill (B)

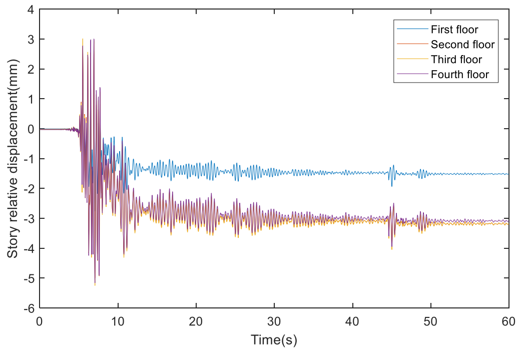

Fig.22 – Story relative displacement of masonry infill (C)

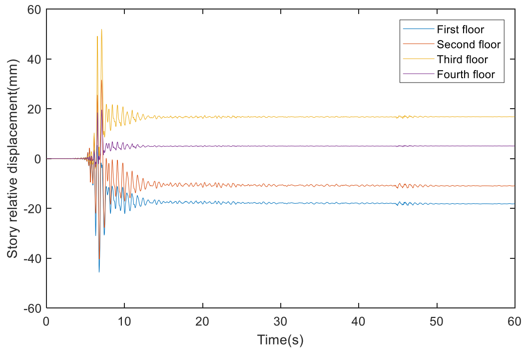

Fig.23 – Story relative displacement of masonry infill (D)

Fig.24 – Damaged masonry infill inside the building

Fig.25 – Damaged masonry infill at the edge (principal) of the building

5.4 The maximum story relative displacement of two FE models

The maximum displacement in the principal direction of masonry infills in (A) position calculated by the two FE model was compared. The maximum displacement of the positive principal direction can be seen at Fig.25, and the maximum displacement of the negative principal direction can be seen at Fig.26.

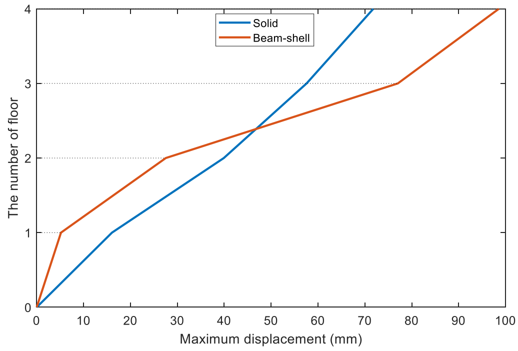

Fig.25 – Maximun displacement of masonry infills in (A) direction (positive)

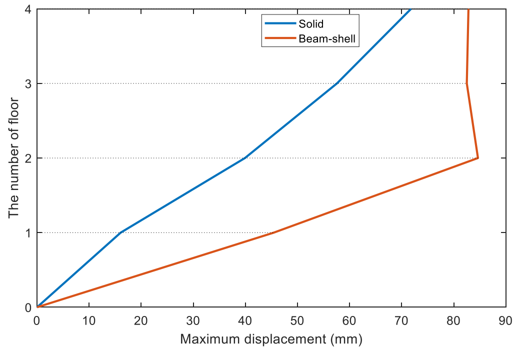

Fig.26 – Maximun displacement of masonry infills in (A) direction (negative)

6. Conclusion

In the Changning earthquake, the non-structural earthquake damage of this teaching building is relatively light, and the ground motion PGA recorded by the nearest station is 599.37 cm/s^2. This paper selects a part of the teaching building and studies this phenomenon through numerical simulation.

In view of this phenomenon, in this paper, the acceleration time history recorded by the nearest station to the teaching building was selected, two kinds of finite element models were established, and modal analysis, seismic response spectrum analysis and elastic-plastic time history analysis were carried out.

The maximum displacement carried out by spectrum analysis of solid FE model is 71.8 mm, and the number carried out by elastoplastic time history analysis of beam-shell FE model is 95.1 mm. According to the actual earthquake damage pictures, the simulation results are consistent with the facts.

7.Acknowledgements

This work is supported by Earthquake Research Fund of CEA (2019EEEVL0402, 2019A03), Heilongjiang Provincial Natural Science Foundation of China (LH2019E094), Program for Innovative Research Team in China Earthquake Administration.

8.Copyrights

9. References

[1] Zhai Changhai, Wang Xiaomin, Kong Jingchang (2018): Research status and Prospect of seismic performance of masonry infilled wall RC frame structure. Journal of Harbin University of technology v.50.06 (2018): 7-19

[2] Zhang Zhaohui (2010): Ansys12.0 structural analysis engineering application example analysis, Third edition. Beijing, China Machine Press.

[3] Li Wei (2006): Application example of ANSYS Civil Engineering (Second Edition), China Water Conservancy and Hydropower Press, Wanshui ANSYS Technology Series.

[4] Shang Xiaojiang, Qiu Feng, Zhao Haifeng etc. (2006): Advanced finite element analysis method and example application of ANSYS structure (First Edition), China Water Conservancy and Hydropower Press, Wanshui ANSYS Technology Series.

[5] Wang Xinmin (2007): Numerical analysis of ANSYS engineering structure, People's Communications Press.

[6] Zhu Lei (2015): The Finite Element Analysis of the Influence of Cast-in-place and Infill-walls on the Seismic Performance of RC Frame Structure, Nanchang Hangkong University.

[7] Lu Xinzheng, Jiang Jianjing (2003): Analysis of complex stress of concrete composite members with ANSYS solid 65 element, Building structure, 2003 (06): 22-24.

[8] ANSYS company, USA: ANSYS Theory Manual, Version 19.0

[9] Ministry of Housing and Urban-Rural Development of the People's Republic of China (2015): Code for design of concrete structures, China Architecture & Building Press.

[10] Yan Hongxia (2012): Influences of Slabs and Infill Walls on Seismic Performance of Reinforced Concrete Frame Structures, Beijing Jiaotong University.

[11] Ministry of Housing and Urban-Rural Development of the People's Republic of China (2015): Code for design of masonry structures, China Architecture & Building Press.

[12] Lin Xuchuan, Lu Xinzheng, Ye lieping (2010): Simulation and analysis of earthquake collapse of masonry structure, Analysis and design of anti-collapse of building and engineering structure, 2010,238-252.

